Effect of springtime thermal forcing over Tibetan Plateau on summertime ozone in Central China during the period 1950–2019

8 authors, including:

Yingying Yan
China University of Geosciences
54 PUBLICATIONS   1,097 CITATIONS

SEE PROFILE

Jintai Lin
Peking University
120 PUBLICATIONS   5,450 CITATIONS

SEE PROFILE

Huang Zheng
China University of Geosciences
48 PUBLICATIONS   512 CITATIONS

SEE PROFILE

Some of the authors of this publication are also working on these related projects:

Project   Greenhouse gases and energy View project

Project   Satellite remote sensing of air pollutants, emissions, and impacts View project

Effect of springtime thermal forcing over Tibetan Plateau on summertime ozone in Central China during the period 1950–2019

Yuexuanzi Wang [a,1], Yingying Yan [a,*,1], Kunyu Duan [a], Shaofei Kong [a,b], Jintai Lin [c], Huang Zheng [a,d], Aili Song [a], Zexuan Zhang [a,d]

[a] Department of Atmospheric Science, School of Environmental Sciences, China University of Geosciences, Wuhan 430074, China
[b] Research Centre for Complex Air Pollution of Hubei Province, Wuhan 430078, China
[c] Laboratory for Climate and Ocean-Atmosphere Studies, Department of Atmospheric and Oceanic Sciences, School of Physics, Peking University, Beijing 100871, China
[d] Department of Environmental Science and Engineering, School of Environmental Studies, China University of Geosciences, Wuhan 430074, China

ARTICLE INFO

ABSTRACT

In recent years, ozone pollution has attracted wide attention from the scientific community, policymakers and the public. Previous studies have already confirmed the effects of meteorological conditions on regional ozone pollution events in the last two decades. However, due to the lack of historical ozone observations, the relationship of climate variability and ozone pollution has been less discussed. In our study, we use the NCEP/NCAR Reanalysis data and modeled historical surface ozone from CMIP6 (Coupled Model Intercomparison Project Phase 6) to explore the impact of climate variability related to Tibetan Plateau on summertime (June, July and August) ozone in Central China during 1950–2019. The results show that in interdecadal timescale, the annual summertime ozone over Central China is significantly correlated ($R = -0.52$; P-value <0.05) with the springtime (March, April and May) thermal forcing, indicated by total atmospheric energy (TPE), over Tibetan Plateau. In high TPE years, the East Asian monsoon (southerly wind flow) and vertical ascending motion have been enhanced in summer. It is conducive to both the diffusion of ozone and its precursors and occurrence of cloudy and high humidity weather. These processes lead to lower ozone concentrations up to 6.97 ppb (compared with values averaged during 1950–2019) over Central China. On the contrary, in low TPE years, summertime surface ozone concentrations have been increased by 2.96 ppb (the mean value is 49.00 ppb and the standard deviation is 11.75 ppb for 1950–2019) on average of Central China, due to the weakened East Asian monsoon and weakened vertical ascent, thus the stable weather with low humidity and small near surface wind. After the year 2000, the TPE has increased with a rapid growth rate of 3×10^4 hPa J kg^{-1} yr^{-1}. However, similar to the reported surface ozone increments based on the modeling results and observations, the CMIP6 summertime surface ozone has shown an increasing trend in the last two decades (0.45 ppb yr^{-1} and 0.25 ppb yr^{-1} over Central China and entire China during 1950–2019, respectively). While a decline trend (0.18 ppb yr^{-1}) of ozone from 1980 to 2019 over Central China is calculated after the removal of emission-attributed trend. These results indicate that the ozone increasing trend dependent on the changes of precursor emissions has offset the ozone mitigation attributed to the climate.

1. Introduction

Tropospheric ozone (O_3) is produced via photochemical oxidation of volatile organic compounds (VOCs) and nitrogen oxides ($NO_x \equiv NO + NO_2$) (Sillman et al., 1990; Shen et al., 2019). It is a vital component in the atmosphere that participates in the oxidation of chemically and climatically relevant trace gases (Lelieveld et al., 2000; Wang et al., 2017), as the strong oxidizing hydroxyl radicals (OH) formatting along with ozone. Surface ozone is one of the serious air pollution issues in China over the past decades (Ma et al., 2012; Ma et al., 2016; Sun et al., 2019; Yan et al., 2021), and its damage to agriculture, forests and grasslands has been reported to be increased (Krupa and Manning, 1988; Tai et al., 2014; Emberson, 2020). It also has a harmful effect on human health, especially leading to premature respiratory mortality (Fu and

Tai, 2015; Lelieveld et al., 2015).

Surface ozone pollution is not only attributed to the anthropogenic emissions of VOCs and NO$_x$, but it is also influenced by meteorological conditions (Emberson, 2020; Fu and Tai, 2015; Yan et al., 2018a; Yan et al., 2019). Temperature, relative humidity, solar radiation and atmospheric circulation are highly correlated with ozone variability (Davies et al., 1992; Jacob and Winner, 2009; Xu and Lin, 2011; Zhang et al., 2015; Wie and Moon, 2016; Kavassalis and Murphy, 2017; Yan et al., 2018b; Xu et al., 2018; Cheng et al., 2019). Cloudless sky, high temperature and low humidity are conducive to the formation of ozone pollution (Duan et al., 2008; He et al., 2017; Jacob and Winner, 2009). In addition to the local meteorological factors, the distribution and variation of ozone are also affected by regional weather conditions controlled by synoptic-scale and large-scale atmospheric circulation (Zhang et al., 2012; Shu et al., 2016; Pu et al., 2017; Liao et al., 2017; Gong and Liao, 2019; Li et al., 2020; Han et al., 2020). These previous studies have emphasized that different levels of local ozone pollution are closely related to the dominant synoptic or atmospheric circulation types in the specific region, which have strong impacts on the dispersion and regional transport of pollutants.

Many studies have also discussed the relationships between ozone and different natural climate systems, such as solar cycle, El Nino Southern Oscillation (ENSO), Quasi-Biennial Oscillation (QBO), Arctic Oscillation (AO) and East Asian Summer Monsoon (EASM) (Zhou et al., 2013; Yang et al., 2014b; Chen et al., 2020). By using the tropospheric column ozone (TCO) datasets of Ozone Monitoring Instrument/Micro wave Limb Sounder (OMI/MLS; 2005–2017) and surface ozone measurements (2006–2016) of 16 observation sites in Southern China, Chen et al. (2020) have shown a large impact on TCO (by 2–7 DU) and on surface ozone (by 3–8 ppb) from solar cycle, while an insignificant effect on tropospheric ozone trends by ENSO, QBO and AO. By analyzing ozone measurements over Hong Kong for 11 years, Zhou et al. (2013) have shown that the interannual variation of ozone is closely related to the East Asian monsoon. By using the GEOS-Chem chemical transport model, Yang et al. (2014b) have also found a statistically significant positive correlation between the intensity of EASM and summertime ozone concentration on average in China during the period of 1986–2006. In Southern China, the Asia summer monsoon contributes to 24.8% and 81.5% of summertime TCO and surface ozone variabilities, respectively (Chen et al., 2020), by influencing the precipitation and wind fields. To investigate the effects of local synoptic conditions and large-scale climate environment on historical surface ozone change is of great significance to accurately assess the trend of ozone pollution in China in the future.

The Tibetan Plateau (TP) is strongly interacted to global atmospheric climate systems (Xu et al., 2013; Yang et al., 2014a; Pepin et al., 2015) due to being as the roof of the world, with an average elevation above 4000 m (almost to the mid-troposphere) and about one sixth (2.5×10^6 km^2) of the total land area of Asia. The TP is referred as a giant air pump in the central-eastern Eurasian and exerts strong thermal forcing on the atmosphere over Asian monsoon region, with an elevated atmospheric heat source (AHS) in summer, while negative AHS in winter (Liu et al., 2009; Yang et al., 2014a; Wu et al., 2017). This mechanism plays an important role in weather and climate over China and regulates the seasonal variation of Asian large-scale atmospheric circulation (Liu et al., 2017; Zhou et al., 2009; Wu et al., 2017). For a long period of time, the thermal forcing over the TP has varied and is an indicator of climate change (especially over China) induced by natural variability and anthropogenic activities (Lau et al., 2010; An et al., 2015; Wu et al., 2017). Xu et al. (2013) have reported that the AHS anomalies in spring over the TP significantly influence the summer precipitation in China. Particularly, with the interdecadal weakening (1973–2003) of the thermal forcing over TP, the EASM was weakening as well, along with a dry-trend belt in the northern-central China and more precipitation in southern China.

Previous studies have also observed that the thermal forcing of the

TP will impact the meteorological factors in some parts of China (Zhao and Chen, 2001; Duan and Wu, 2005; Wang et al., 2014; Ge et al., 2019). Thus the distribution, variation and trend of air pollution have a close linkage with the thermal forcing of the TP (Xu et al., 2016; Zhao et al., 2020). Xu et al. (2016) have indicated that the wintertime haze over central-eastern China (CEC) is highly correlated with the AHS of the TP. When TP gets warmer, there are frequent haze events in CEC, as a result of a weakened winter monsoon and an increased atmospheric stability. While the warming TP improves winter air quality in Sichuan Basin, due to the enhancement of easterly wind and planetary boundary layer height (PBLH) and the decline of relative humidity (RH) in the basin (Zhao et al., 2020). In addition, many previous studies have confirmed that the springtime TP thermal forcing will strongly influence the atmospheric circulation and precipitation over China in the following season (Zhao and Chen, 2001; Duan and Wu, 2005; Zhao et al., 2007; Duan et al., 2011; Xu et al., 2013; Wang et al., 2014; Cui et al., 2015; Ge et al., 2019). To explore the effects of springtime thermal forcing of TP on the forthcoming meteorological factors and then surface ozone is of great significance to improve the accuracy of ozone pollution prediction.

In this study, we will explore the impact of climate variability indicated by the thermal forcing of Tibetan Plateau on historical summertime surface ozone for the period of 1950–2019 over Central China (108–118°E, 24–36°N). Central China is located in the downstream of the TP and remarkably influenced by the thermal forcing. For its special geographical position, it is a regional pollutant transport hub with sub basin topography (Zheng et al., 2019; Yu et al., 2020; Shen et al., 2021; Yan et al., 2021). In addition, Central China has increasingly suffered severe ozone pollution due to high precursor anthropogenic emissions (Zeng et al., 2018). Firstly, we use the NCEP/NCAR Reanalysis dataset to calculate the annual springtime total atmospheric energy (TPE) over the TP. Then we discuss the relationship between the high/low TPE years and the difference of meteorological conditions in summer over Central China. Finally, the effects of climate variability indicated by the TPE of Tibetan Plateau on summertime ozone are evaluated by CMIP6 historical ozone simulations in Central China.

2. Data and methods

2.1. Data

We use the monthly mean reanalysis data (with a horizontal resolution of 2.5° longitude × 2.5° latitude and 17 vertical layers) generated by the National Centers for Environmental Prediction/National Center for Atmospheric Research (NCEP/NCAR; https://psl.noaa.gov/data/gridded/data.ncep.reanalysis.pressure.html/). This dataset has been evaluated by previous studies (Decker et al., 2012; Bracegirdle and Marshall, 2012; Xu et al., 2013) and has been widely used to analyze the global and regional climate variability and its affecting factors and impacts (Wang et al., 2010; Bromwich et al., 2011; Garreaud et al., 2013; Woollings et al., 2015; Li et al., 2016; Butler et al., 2017). In order to evaluate whether NCEP/NCAR reanalysis data is suitable for this work, we also use the monthly averaged data on pressure levels (with a horizontal resolution of 0.25° longitude × 0.25° latitude) generated by European Centre for Medium-Range Weather Forecasts (ERA5; https://www.ecmwf.int/en/forecasts/datasets/reanalysis-datasets/era5/) to conduct a comparison (see details in supplementary section 1).

Due to the lack of historical ozone observations, we use the modeled hourly surface ozone (SFO3; 1950–2019; 1.25° longitude × 1.25° latitude) from CMIP6 (https://cera-www.dkrz.de/WDCC/ui/cerasearch/cmip6?input=CMIP6.CMIP.MOHC.UKESM1-0-LL.historical/). Moreover, in order to conduct a model-observation comparison, we use the ozone satellite retrieval data (2005–2017; 0.25° longitude × 0.25° latitude) from the space-based Ozone Monitoring Instrument (https://www.cfa.harvard.edu/atmosphere/) and in-situ observation data from the China's Ministry of Ecology and Environment (https://data.cma.cn/). The modeled summertime SFO3 (modeled surface ozone

data from the CMIP6) over Central China has reproduced the spatial distribution of observed near surface ozone from both in-situ measurements and retrieved from OMI (satellite retrieval surface ozone data from the space-based Ozone Monitoring Instrument) (Fig. S1), although an underestimation over Northern China Plain and an overestimation over Western China are found. The correlation coefficients between re-gridded modeled surface ozone data (SFO3) and measured ozone (OMI; MEE: in-situ observation surface ozone from the China's Ministry of Ecology and Environment) are statistically significant (Fig. 1; *P*-value <0.05). Specifically, correlation coefficient between SFO3 (from 1.25° × 1.25° to 0.25° × 0.25°) and OMI from 2005 to 2017 over the entire China is 0.46. Also, the correlation coefficient of 2016–2019 SFO3 (from 1.25° × 1.25° to 1° × 1°) and MEE (from station coordinate to 1° × 1° by spatial interpolation method; noontime ozone between 12:00 and 15:00 based on 8-h moving averages) is 0.26. In addition, the trend of modeled SFO3 over Central China during the period 2005–2019 is consistent with that detected from merged ozone measurements (Fig. 1). In order to evaluate the OMI ozone, we have added a comparison between OMI and MEE in the period 2016–2017. The results show that they are significantly correlated, with $R = 0.81$ (P-value <0.05) (Fig. S2). Moreover, the modeled historical surface ozone we used is highly correlated with four long-term observational stations, especially significantly correlated with the station of Mauna Loa, Hawai'i, USA (MLO, 19.5°N, 155.6°W, 11 m.a.s.l., 1957–present), with a temporal correlation of 0.74 and a mean normalized bias error of 2.5%. (Griffiths et al., 2021).

In order to exclude the effects of anthropogenic emission changes on surface ozone trend, we use a statistical model of Kolmogorov-Zurbenko (KZ) filter (Seo et al., 2018) to differentiate the anthropogenic effects from the contribution of climate variability (see details in supplementary section 2). The KZ filter method indicates that the surface ozone long-term trend (0.45 ppb yr^{-1} and 0.25 ppb yr^{-1} over Central China and entire China during 1950–2019, respectively; Fig. S3) is mainly contributed by anthropogenic emissions, while there is small trend in time series of meteorological-contributed ozone (Fig. S4). We use the time series of annual summertime ozone after removal of emission-attributed trend to analyze the effects of climate variability in the following text.

2.2. The thermal forcing of Tibetan Plateau

We calculate the atmospheric energy of each layer over Tibetan Plateau (25–37.5°N, 80–105°E) by the following formula:

$$TPE = E_s + E_p + E_k + E_L = c_p T + gz + \frac{1}{2}V^2 + Lq$$

Here, E_s is the sensible heat energy, E_p indicates the geopotential energy, E_k is defined as the kinetic energy, and E_L represents the latent energy. Then the column-integrated total atmospheric energy in the troposphere from 1000 hPa to 300 hPa is calculated to characterize the thermal forcing of Tibetan Plateau by:

$$TPE = -c_p \int_{P_0}^{P_1} T dp + g \int_{P_0}^{P_1} z dp + \frac{1}{2} \int_{P_0}^{P_1} V^2 dp - L \int_{P_0}^{P_1} q dp$$

where T is the air temperature, z is the geopotential height, V = (u, v) indicates the horizontal wind vector, p is the pressure, and q is the specific humidity. p_0 and p_1 are the first layer (1000 hPa) and the layer of tropopause (300 hPa), respectively. In addition, c_p represents the specific heat capacity of air at constant pressure (1.0 KJ kg^{-1} K^{-1}), g is the gravitational acceleration (9.8 m s^{-2}) and L is defined as the latent heat of water vaporization (2257.2 KJ kg^{-1}).

From April to September, the Tibetan Plateau acts as a heat source. Using the monthly averaged meteorological data (1961–1995), Zhao and Chen (2001) have indicated that the strongest atmospheric heat source is in June (78 W m^{-2}). Here we calculate the springtime TPE of Tibetan Plateau to explore the climate effects on summertime surface ozone over Central China, due to the time-lagged impact of spring heat source over the TP on the summer meteorological anomaly in Central and East China. The springtime TP thermal forcing has been confirmed as an important factor that influences the Asian summer monsoon and rainfall belt in central and eastern China (Zhao and Chen, 2001; Zhao
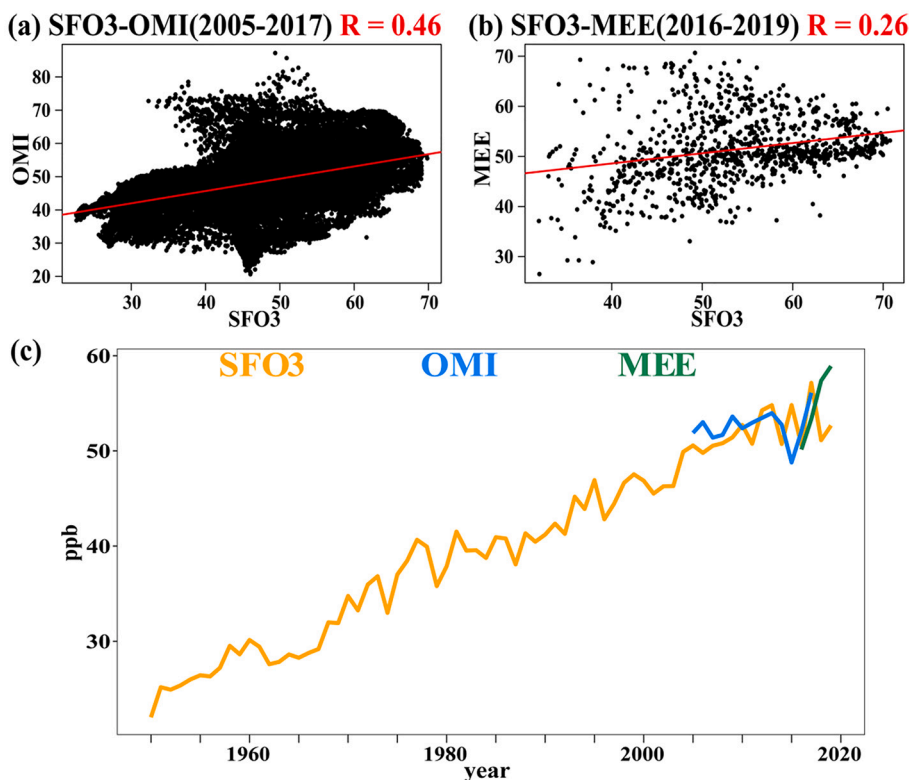

Fig. 1. (a) The correlation between SFO3 (modeled surface ozone data from the CMIP6) and OMI (satellite retrieval surface ozone data from the space-based Ozone Monitoring Instrument) over entire China from 2005 to 2017 ($R = 0.46$, *P*-value <0.05). (b) The correlation between SFO3 and MEE (in-situ observation surface ozone from the China's Ministry of Ecology and Environment) over entire China from 2016 to 2019 (R = 0.26, P-value <0.05). (c) Time series of annual mean summertime surface ozone concentration in Central China (108–118°E, 24–36°N) from 1950 to 2019.

et al., 2007; Duan et al., 2011; Xu et al., 2013; Wang et al., 2014; Cui et al., 2015; Ge et al., 2019). For instance, Duan and Wu, 2005 have used the NCEP/NCAR Reanalysis diagnosis to indicate that the stronger the TPE over Tibetan Plateau in spring is, the more rainfall will happen in the following July over the Yunnan-Guizhou Plateau and the middle reaches of the Yangtze River and Huaihe River, while in the North and South China will be less than normal. The results imply the relationship between TPE and the atmospheric circulation as well as the precipitation in the forthcoming season.

In order to find the high/low TPE years, we compute the fitted average by locally weighted linear regression method and the mean value of TPE, respectively (Fig. 2). When the fitted average of TPE > the mean value of TPE, we define the year as high TPE year (HY). When the fitted average of TPE < the mean value of TPE, we define the year as low TPE year (LY).

3. Results

3.1. Springtime thermal forcing of Tibetan Plateau during the period 1950–2019

Fig. 2 shows the time series of annual springtime total atmospheric energy over Tibetan Plateau from 1950 to 2019. The fitted average of TPE depicts the interdecadal trend of climate variability. There is a slight upward tendency from the year 1950, and the TPE reaches a maximum of 7.17×10^7 hPa J kg^{-1} in 1969. Then it gradually descends, with the minimum value of 6.93×10^7 hPa J kg^{-1} in 2000. After 2000, there is a rapid increasing trend, and the maximum TPE is 7.17×10^7 hPa J kg^{-1} in 2016. Thus the time series of TPE can be effectively divided into three periods: 1950–1969 (upward), 1970–2000 (downward) and 2001–2019 (upward). The trends are 1.1×10^5 hPa J kg^{-1} yr^{-1}, -0.4×10^5 hPa J kg^{-1} yr^{-1}, 0.3×10^5 hPa J kg^{-1} yr^{-1}, respectively. Zhao and Chen (2001) have also shown a decreasing trend of springtime thermal forcing of the TP since 1960s investigated by 1961–1995 monthly meteorological observation data from 148 stations. Moreover, our results of TPE change are similar to the study of Xu et al. (2013), which has used the springtime NCEP/NACR Reanalysis data (1950–2010) to divide the TPE into three periods: 1950–1973 (upward), 1973–2003 (downward) and 2003–2010 (upward). From 1980s to 2000s, the Tibetan Plateau have experienced surface air warming, humidifying, solar dimming, and wind
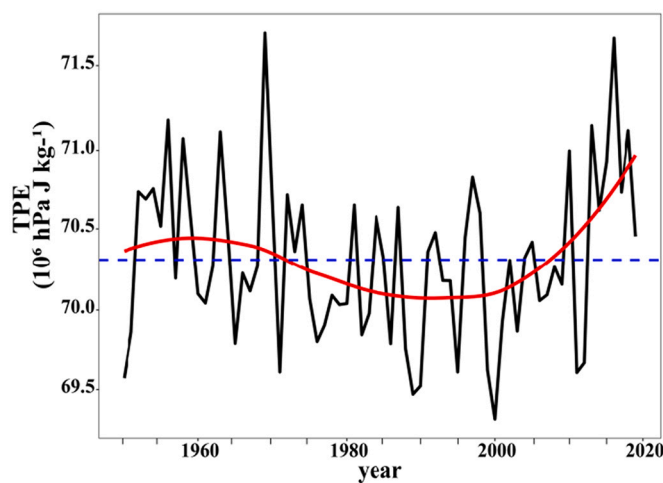

Fig. 2. Time series of springtime TPE (10^6 hPa J kg^{-1}) over the TP from 1950 to 2019 (black curve). The fitted average of TPE is marked by the red curve, depicting the interdecadal trend. The mean value of TPE is marked by the blue dotted line, which is the marks to distinguish the high TPE years (fitted average > mean value) and low TPE years (fitted average < mean value), respectively. (For interpretation of the references to colour in this figure legend, the reader is referred to the web version of this article.)

stilling (Yang et al., 2014a). The warmer and more humid air will form more clouds, which will lead to solar dimming and reduce solar radiation received by the surface. In addition, the surface sensible heat will decrease. Since the surface has received less heat and radiation, and the still wind has slowed down the transportation, the Tibetan Plateau has less atmospheric energy in this period.

Then, we use the fitted average and the mean value of TPE to define the high/low TPE years (Fig. 2). The high TPE years (HY) with the fitted average > the mean value are 1950–1971 and 2010–2019, while the low TPE years (LY) are from 1972 to 2009.

3.2. Effects of the thermal forcing on summertime meteorological factors over Central China

To investigate the influence of springtime thermal forcing on summertime meteorological factors over Central China, we calculate the differences of meteorological fields averaged over the study period (1950–2019) and the high/low TPE years over Central China. The meteorological variables we discussed are from 1950 to 2019, including surface air temperature (1000 hPa), specific humidity (1000 hPa), horizontal wind fields (1000 hPa, 850 hPa and 500 hPa), and vertical velocity (1000 hPa, 850 hPa and 500 hPa).

The differences of horizontal wind fields are shown in Fig. 3. Averaged over the period 1950–2019, the East Asian summertime monsoon (southerly wind flow) is clearly visible (Fig. 3a), with the average wind speed of 3.40 m/s at 850 hPa over Central China. For the HY, we find anomalous southerly flow, especially at 850 hPa in the area of Central China. While in the LY, anomalous northerly flows are shown over Central China. The average anomalous wind speeds over Central China are 0.99 m/s and − 0.93 m/s at 850 hPa in high and low TPE years, respectively (Table 1). The results indicate that the East Asian summer monsoon is enhanced in the HY and weakened in the LY. Ding et al. (2008) have shown that the East Asian summer monsoon is related to the summer precipitation in China. Our results are consistent with previous studies and show that when the EASM has become weaker, the north and northeast of China suffer severe and persistent drought, while the Yangtze River Basin and South China experience much more severe heavy rainfall/flood events (Fig. S5).

In addition, the 1000 hPa vertical velocity over the most part of Central China is anomalous negative in the HY, while anomalous positive in the LY (Fig. 4). The average vertical velocity is 42.02% (35.53%) lower (higher) in the HY (LY). However, for the HY (LY), as shown in the 850 hPa and 500 hPa, the vertical velocity becomes anomalous positive (negative) in the southern part of Central China. The average vertical velocity is 13.62% and 2.98% (15.96% and 3.48%) higher (lower) in the HY (LY) at 850 hPa and 500 hPa, respectively (Table 1). These results show that there are stronger instable air convection and convergence upward movement in low troposphere over Central China in the HY. By contrast, due to the weakened ascending air flow and enhanced vertical subsidence in low layers and the enhanced vertical upward motion in high layers, the atmospheric environment is more stable over Central China in the LY.

The results of horizontal wind fields and vertical velocity illustrate that the Tibetan Plateau sensible heat works as an air pump (TP-SHAP) and regulates the atmospheric circulation from the lower troposphere to the upper troposphere (Wu et al., 2007), which significantly impacts the climate variability over Central China. In the HY (Fig. S6), the TP-SHAP is stronger, and the thermal adaptation results in weak cyclonic circulation near the surface and strong anticyclonic circulation in the surface layer over TP (Duan and Wu, 2005), significantly enhancing the local monsoonal meridional circulation and intensifying the lower layer's south air flow over the Asian monsoon area (Wu et al., 2016), especially over Central China. By contrast, in the LY (Fig. S7), the southern wind and the vertical ascending motion are much weaker, making the atmospheric stability stronger. Therefore, both of the horizontal wind fields and the vertical velocity anomalies are concordance to the anomaly of
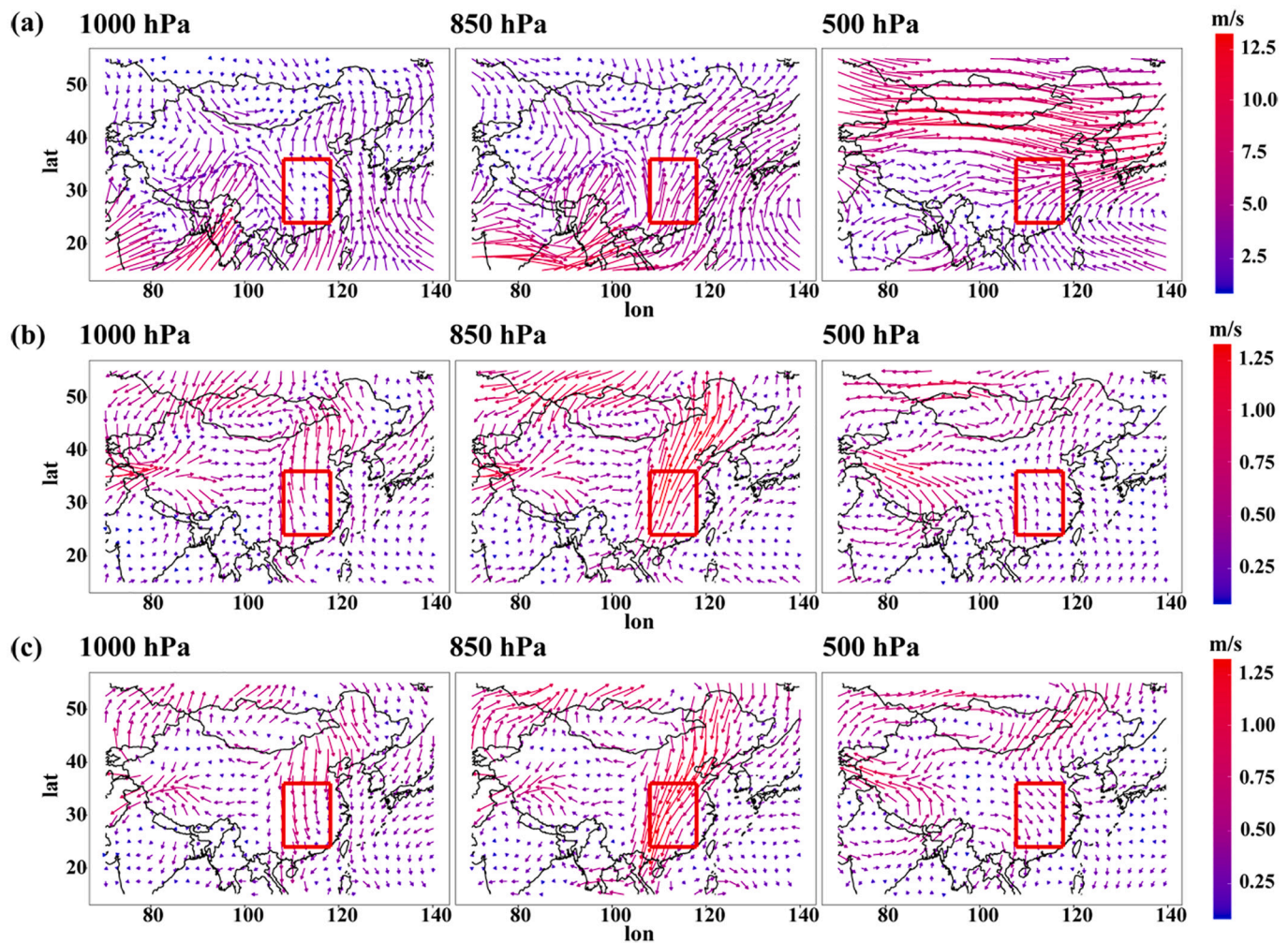
Fig. 3. The spatial distribution of horizontal wind fields at 1000 hPa, 850 hPa and 500 hPa (a). The differences of summertime horizontal wind fields averaged over the study period (1950–2019) and the high/low (b/c) TPE years at 1000 hPa (P-value = 0.20/0.21), 850 hPa (P-value = 0.04/0.10) and 500 hPa (P-value = 0.42/0.46). The red frame draws the area of Central China. (For interpretation of the references to colour in this figure legend, the reader is referred to the web version of this article.)

Asian monsoon, relating to the total energy over Tibetan Plateau.

The effects of thermal forcing on summertime surface air temperature and specific humidity are shown in Fig. 5. To avoid the impact of global warming on surface air temperature, we use the detrended reanalysis 1000 hPa air temperature data to conduct analysis. The removed long-term trend (0.02 °C yr^{-1}) is according to the V3.3 Remote Sensing Systems lower-tropospheric temperature series (http://www.remss.com/data/msu/monthly_time_series/; over the fully sampled global landmass in 1979–2008) (Parker, 2011). After the removal of long-term trend in surface air temperature, a clear positive (negative) difference over Central China can be seen in the HY (LY). The averaged difference between the HY (LY) and the period 1950–2019 is 0.12 °C (−0.15 °C), which is much greater than the influence of global warming on temperature. The 1000 hPa specific humidity (Fig. 5) is higher (20.00 versus 19.87 g kg^{-1}) in most area of Central China in the HY than that averaged over 1950–2019, whereas lower (19.75 versus 19.87 g kg^{-1}) in the LY (Table. 1).

The warming Tibetan Plateau promotes upward movement of sensible heat flux, which induces convection and more precipitation. At the same time, the precipitation releases more latent heat, which strengthens the South Asian High (Rodwell and Hoskins, 2010). As a result, the westerly jet flow at north TP and the easterly jet flow at south TP become stronger in upper troposphere. Meanwhile, there is a downward flow at northwest TP and an upward flow at northeast TP,

which enhance more precipitation in East Asian region, further strengthen the East Asia monsoon (Wang et al., 2008b). Shi et al. (2008) have also demonstrated that the thermal forcing over the TP significantly enhances the surface heat flux and the general eastward propagation of heat source to China. Moreover, the monsoonal airflow is related to the West Pacific subtropical high (Ding and Chan, 2005; Wang et al., 2008a), which brings warm air full of water vapor, and then results in rainfall. In brief, the higher the TPE is, the stronger the heat flux transports, the stronger the EASM is, the more the specific humidity is, the stronger the latent heat of water is, the higher the surface air temperature is (Fig. S8).

3.3. Effects of the thermal forcing on summertime ozone over Central China

In our study, after removing the emission-attributed trend, we focus on the effects of meteorological factors affected by thermal forcing over the TP on the ozone formation and transportation over Central China. The difference of detrended summertime surface ozone averaged over the study period (1950–2019) and the high/low TPE years is shown in Fig. 6. In the HY, ozone mixing ratios are much lower than climatological annual mean concentrations (49.00 ppb for 1950–2019), with the maximum difference being up to 6.97 ppb (14.22%). However, averaged over Central China, ozone concentration in the LY is higher

Table 1

The statistics of summertime meteorological factors (surface air temperature, specific humidity, horizontal wind speed and vertical velocity) and ozone concentrations averaged over the study period (1950–2019) and the high/low TPE years over Central China.

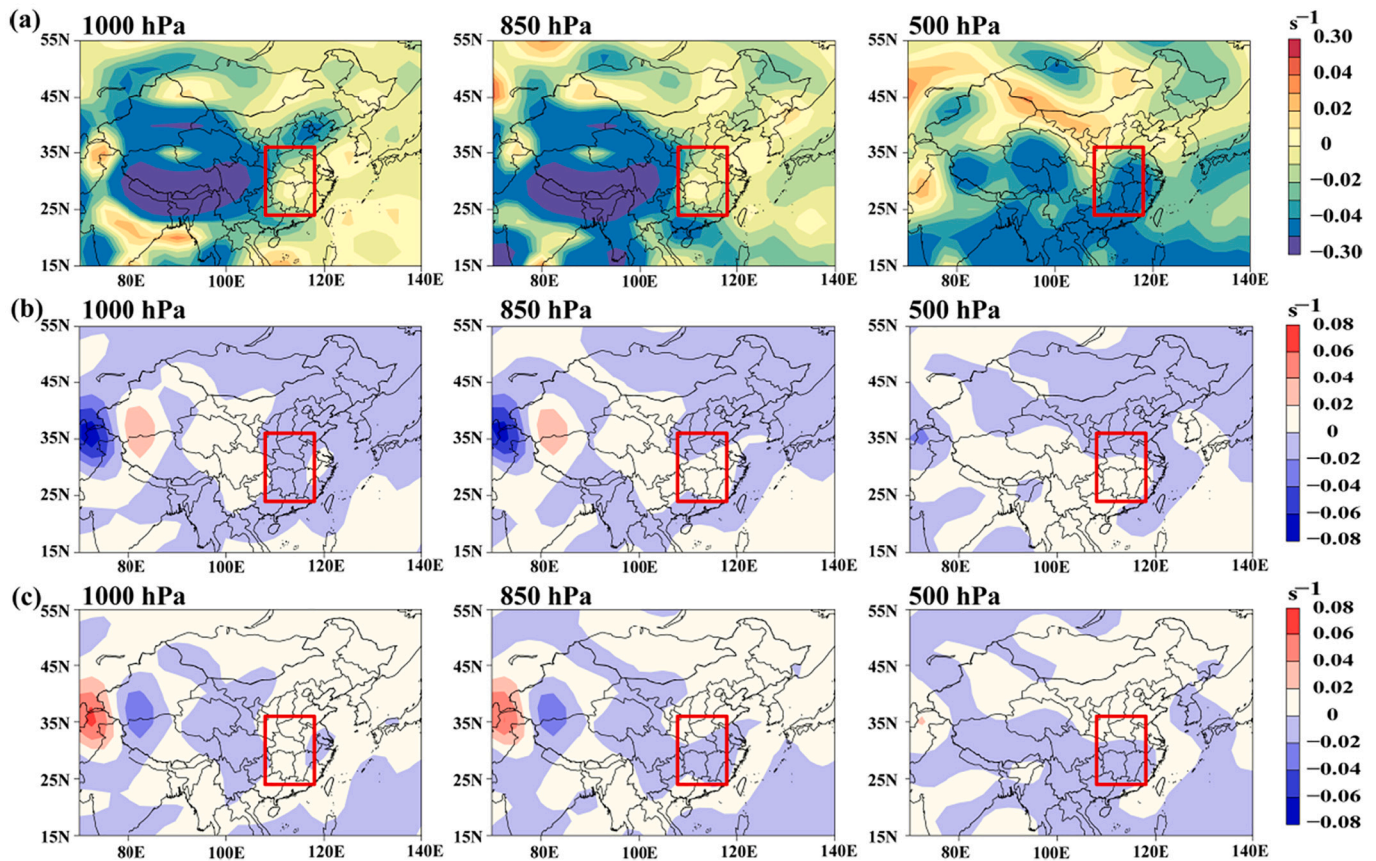| Variable	1950–2019			High TPE years			Low TPE years		
	Max	Min	Ave	Max	Min	Ave	Max	Min	Ave
Surface air temperature (°C)	27.39	24.27	26.04	27.60 (0.21; 0.77%)	24.21 (−0.06; −0.25%)	26.16 (0.12; 0.46%)	27.14 (−0.25; −0.91%)	24.21 (−0.06; −0.25%)	25.89 (−0.15; −0.58%)
specific humidity (g kg^{-1})	21.57	15.67	19.87	21.65 (0.08; 0.37%)	15.94 (0.27; 1.72%)	20.00 (0.13; 0.65%)	21.55 (−0.02; −0.09%)	15.36 (−0.31; −1.98%)	19.75 (−0.12; −0.60%)
1000 hPa wind speed (m/s)	2.23	0.60	1.44	2.67 (0.44; 19.73%)	0.93 (0.33; 55.00%)	1.87 (0.43; 29.86%)	2.01 (−0.22; −9.87%)	0.12 (−0.48; −80.00%)	1.04 (−0.40; −27.78%)
850 hPa wind speed (m/s)	5.55	2.14	3.40	6.72 (1.17; 21.08%)	2.82 (0.68; 31.78%)	4.39 (0.99; 29.12%)	4.41 (−1.14; −20.54%)	1.13 (−1.01; −47.20%)	2.47 (−0.93; −27.35%)
500 hPa wind speed (m/s)	7.56	2.49	4.86	7.47 (−0.09; −1.19%)	2.48 (−0.01; −0.40%)	4.87 (0.01; 0.21%)	7.85 (0.29; 3.84%)	2.19 (−0.30; −12.05%)	4.97 (0.11; 2.26%)
1000 hPa omega speed (10^{-3} s^{-1})	5.12	−33.61	−11.09	2.84 (−2.28; −44.53%)	−42.58 (−8.97; −26.69%)	−15.75 (−4.66; −42.02%)	9.57 (4.45; 86.91%)	−25.37 (8.24; 24.52%)	−7.15 (3.94; 35.53%)
850 hPa omega speed (10^{-3} s^{-1})	7.42	−27.65	−8.52	11.80 (4.38; 59.03%)	−33.20 (−5.55; −20.07%)	−7.36 (1.16; 13.62%)	3.35 (−4.07; −54.85%)	−22.56 (5.09; 18.41%)	−9.88 (−1.36; −15.96%)
500 hPa omega speed (10^{-3} s^{-1})	−0.62	−62.46	−37.95	−4.39 (−3.77; −608.06%)	−57.29 (5.17; 8.28%)	−36.82 (1.13; 2.98%)	3.19 (3.81; 614.52%)	−67.16 (−4.70; −7.52%)	−39.27 (−1.32; −3.48%)
Suface ozone concentration (ppb)	71.13	31.70	49.00	65.37 (−5.76; −8.10%)	30.07 (−1.63; −5.14%)	45.50 (−3.50; −7.14%)	75.97 (4.84; 6.80%)	33.05 (1.35; 4.26%)	51.96 (2.96; 6.04%)

Fig. 4. The spatial distribution of vertical velocity at 1000 hPa, 850 hPa and 500 hPa (a). The difference of summertime vertical velocity averaged over the study period (1950–2019) and the high/low (b/c) TPE years at 1000 hPa (P-value = 0.33/0.40), 850 hPa (P-value = 0.66/0.70) and 500 hPa (P-value = 0.78/0.86). The red frame draws the area of Central China. (For interpretation of the references to colour in this figure legend, the reader is referred to the web version of this article.)
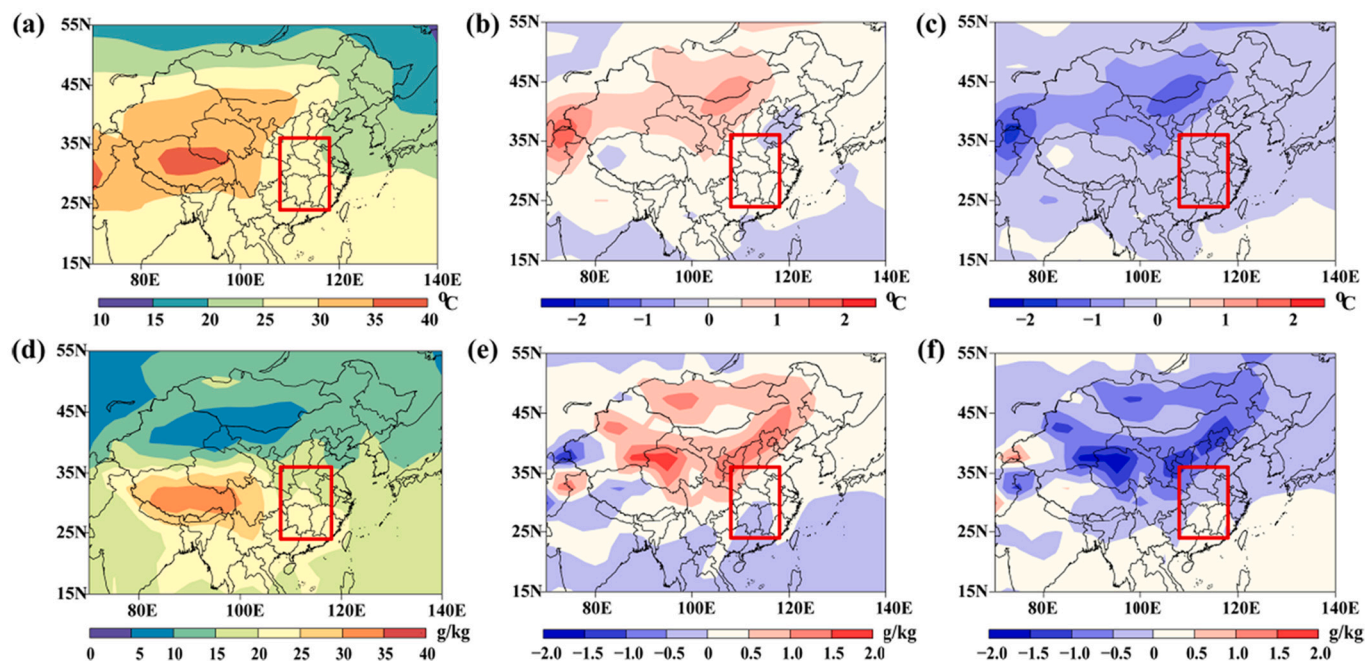
Fig. 5. The spatial distribution of surface air temperature at 1000 hPa (a). The difference of summertime surface air temperature averaged over the study period (1950–2019) and the high/low (b/c) TPE years (P-value = 0.40/0.34). The spatial distribution of specific humidity at 1000 hPa (d). The difference of summertime specific humidity averaged over the study period (1950–2019) and the high/low (e/f) TPE years (P-value = 0.58/0.60). The red frame draws the area of Central China. (For interpretation of the references to colour in this figure legend, the reader is referred to the web version of this article.)

(6.04%; 2.96 ppb) than the climatological annual mean ozone mixing ratio (Table 1). Such low (high) level ozone concentrations in the high (low) TPE years are attributed to the meteorological conditions unfavorable (favorable) to the photochemical formation of ozone but also favorable (unfavorable) to the ozone and its precursors diffusion.

As analyzed in Sect. 3.2, in the HY, there are enhanced EASM, stronger shallow air convection and upward movement, higher surface air temperature and specific humidity over Central China in summer. The strong southwest wind is not only conducive to the ozone diffusion, making against the local ozone accumulation, but also favorable to the pollutant dispersion of ozone precursors, leading to low-level ozone concentrations. In addition, the vertical ascending air in Central China brings ozone and its precursors to the higher layer of troposphere, which is further beneficial to diffuse in atmosphere. Furthermore, the enhanced EASM carries a large amount of warm and humid airflow from the ocean to Central China. Although the temperature rises, the photochemical generation efficiency of ozone decreases due to the frequent occurrence of cloudy and rainy weather (Jiang et al., 2012). These processes lead to lower ozone concentrations by 3.50 ppb (compared with values averaged during 1950–2019) on average of Central China. On the contrary, in the LY, summertime surface ozone concentrations have been increased up to 5.87 ppb (49.00 ppb for 1950–2019) over Central China (Fig. S9). The enhanced ozone is attributed to the weakened East Asian monsoon and weakened vertical ascent in low troposphere, thus the stable weather with low humidity and small near surface wind. These meteorological conditions will enhance the photochemical formation of ozone and local accumulation of pollutants.

The time series of detrended annual summertime ozone concentration averaged over the area of Central China is shown in Fig. 7. From 1950 to 1980, the ozone concentrations have a general increasing trend (0.23 ppb yr^{-1}), and reach the maximum as 28.06 ppb in 1977. After 1980, although there is a slight pick-up around 2000, the overall ozone mixing ratios show a decreasing trend (0.18 ppb yr^{-1}), with the minimum ozone concentration as 20.07 ppb being in 2018.

In order to discuss the problem that in which timescale the connection between the springtime TP heating and the summertime ozone of

Central China is robust, we have also analyzed the correlations of the annual springtime TP heating and annual summertime ozone of Central China to show their connection on an interannual timescale. The correlations between the time series of annual summertime meteorological factors (Fig. 8) and annual springtime TPE (Fig. 2) over the TP are weak, with the correlation coefficients of 0.07, 0.07 and − 0.15 (P-value are 0.58, 0.58, and 0.23, respectively). In addition, the annual summertime ozone (Fig. 7) is weakly correlated with the time series of annual summertime surface air temperature ($R = -0.06$; P-value = 0.61), specific humidity ($R = 0.03$; P-value = 0.78) and vertical velocity ($R = 0.17$; P-value = 0.15) over Central China (Fig. 8). Therefore, the annual summertime ozone of Central China has a relatively weak linkage ($R = -0.13$; P-value = 0.29) with the annual springtime TPE. However, after fitting, the correlations are significant (P-value <0.05). The correlation coefficients between fitted annual summertime ozone (Fig. 7) and fitted annual summertime surface air temperature, specific humidity or vertical velocity are −0.73, −0.88 or 0.44, respectively (Fig. 8). In addition, the correlation coefficients between the fitted summertime meteorological factors (Fig. 8) and fitted springtime TPE (Fig. 2) are 0.48, 0.66 and − 0.70, respectively. Thus, the fitted summertime ozone of Central China is significantly correlated with the fitted springtime TPE ($R = -0.52$; P-value << 0.05). Our results show that the correlation between the TP heating and ozone of Central China on an interdecadal timescale is more robust than that on an interannual timescale. It is noted that further analysis is needed to verify this conclusion with the meteorological field and ozone data from one model, which is not achieved in this study due to the missing data of meteorological data provided by the model in the lower levels over the TP affected by the topography (Fig. S10).

4. Discussion and conclusions

Many previous studies have already investigated the effects of meteorological conditions on summertime high-level ozone pollution events in the last two decades. However, the linkage between climate variability and ozone levels has been less discussed as the lack of
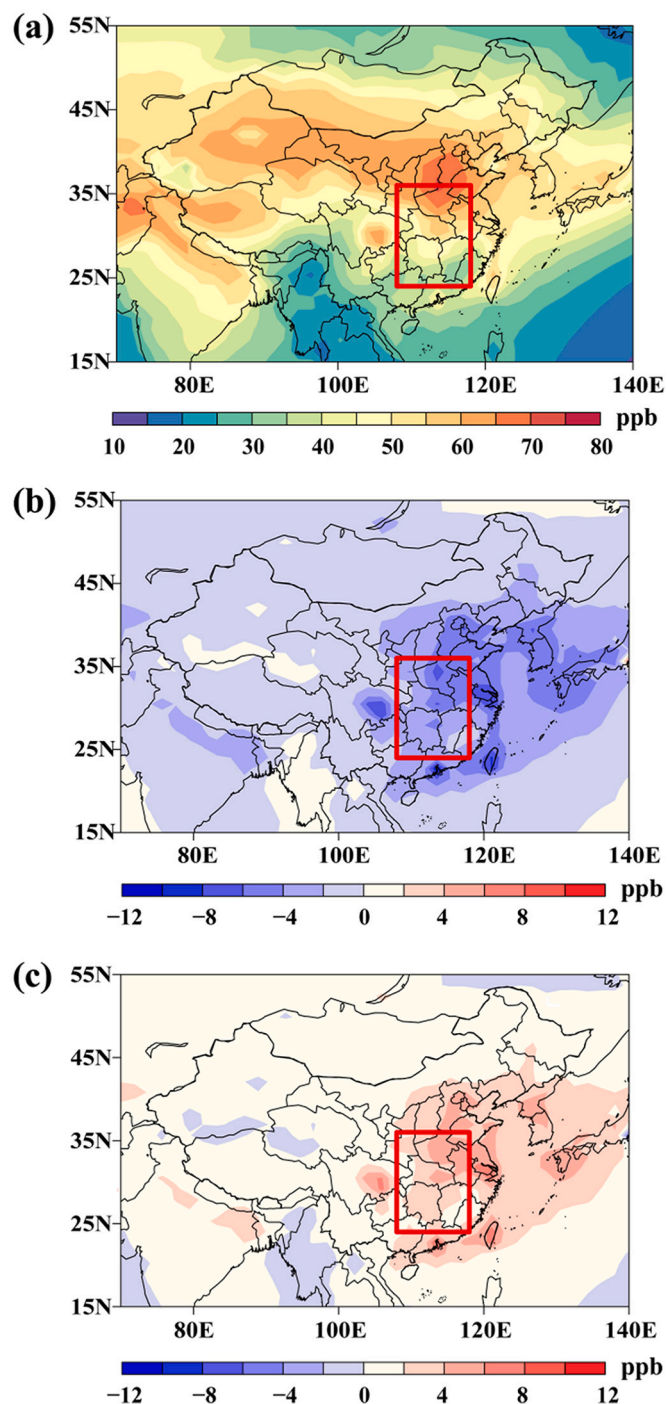
Fig. 6. The spatial distribution of detrended summertime surface ozone concentration (a). The difference of detrended summertime surface ozone averaged over the study period (1950–2019) and the high/low (b/c) TPE years (P-value = 0.01/0.05). The red frame draws the area of Central China. (For interpretation of the references to colour in this figure legend, the reader is referred to the web version of this article.)

Fig. 7. The time series of detrended annual summertime SFO3 in the period 1950–2019 over Central China. The fitted average of SFO3 is marked by the red curve, depicting the interdecadal trend. (For interpretation of the references to colour in this figure legend, the reader is referred to the web version of this article.)

historical ozone datasets, especially over China. Our study explores the effects of climate variability indicated by the thermal forcing of Tibetan Plateau on summertime ozone in Central China during the period of 1950–2019, using the NCEP/NCAR Reanalysis data and modeled historical surface ozone from CMIP6 simulations. The results show that, in interdecadal timescale, there is a significant correlation between annual summertime ozone of Central China after removing emission-related trend and the springtime thermal forcing, indicated by total
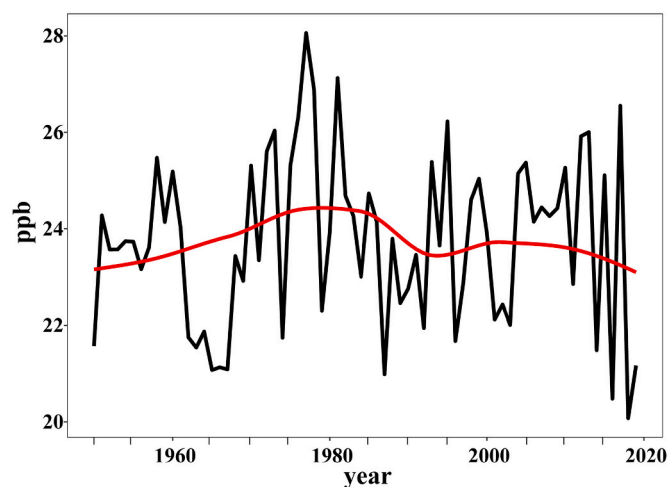
atmospheric energy, of Tibetan Plateau. The effects of the thermal forcing on ozone over Central China can be explained by the impacts of Tibetan Plateau on the meteorological factors in the downstream area. With the increase of springtime thermal forcing, the East Asian monsoon and vertical ascending motion will be strengthened in summer, leading to the southerly air flow deeper and further with more warm air full of water vapor from the ocean to Central China. Thus the ozone concentrations decrease in Central China, for that the meteorological factors are favorable to the diffusion of ozone and its precursors and unfavorable to the photochemical formation efficiency of ozone. By contrast, with the decrease of springtime thermal forcing, the East Asian monsoon and vertical ascent are weakened. As a result, the atmospheric stability is increased with low humidity and small near surface wind, leading to higher summertime surface ozone concentrations on average of Central China.

Our results show that the thermal forcing of Tibetan Plateau can remarkably impact the large scale atmospheric circulation, especially the East Asian summer monsoon, which are consistent with the previous studies (Harris, 2006; Zhao et al., 2007; Duan et al., 2011). The climate variability has been widely recognized as an important role in deciding the regional atmospheric environment, since both the formation and transportation of air pollutants have strong relevance to its affected meteorological conditions. For example, the interannual to decadal variations of winter haze in North China have a strong response to external forcing factors (e.g., the sea surface temperature in the Pacific and Atlantic, snow cover, soil moisture, etc.) (Zhang et al., 2020). While the wintertime haze over central-eastern China and Sichuan Basin are highly correlated to the thermal forcing of Tibetan Plateau (Xu et al., 2016; Zhao et al., 2020). In addition, over large regions of the U.S., the ongoing changes in climate are expected to favor formation of ground-level ozone and thus aggravate associated health and environmental impacts, by altering atmospheric chemistry and transport (Jacob and Winner, 2009).

Our results show that, in Central China, the surface ozone concentration is significantly affected by local meteorological conditions that are further influenced by the large-scale atmospheric circulation related to the thermal forcing of Tibetan Plateau. After removing the emission-related trend (0.45 ppb yr^{-1}), the interannual to decadal variations (up to 6.97 ppb) in summertime ozone levels on average of Central China due to the fluctuations in thermal forcing of Tibetan Plateau are remarkable. In the last two decades, a prominent growth rate of 0.3×10^5 hPa J kg^{-1} yr^{-1} is shown in the springtime thermal forcing over
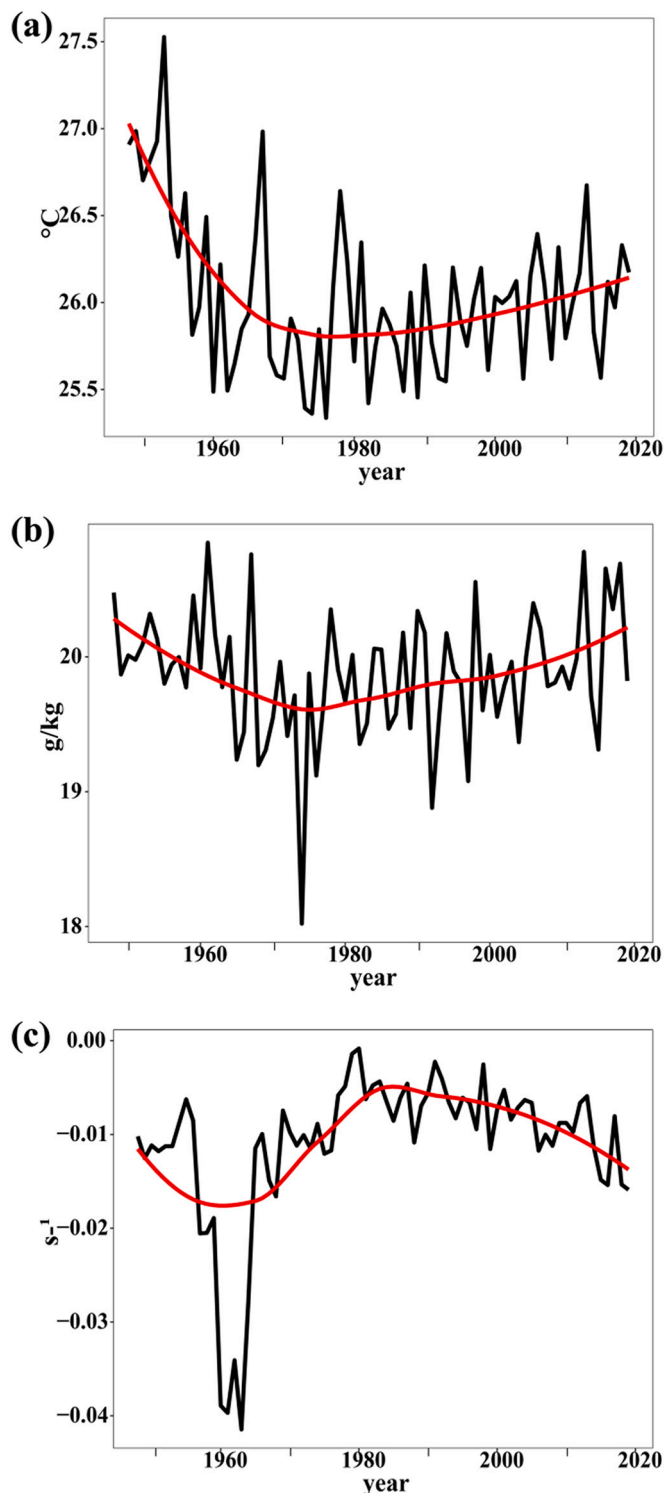
Fig. 8. The time series of summertime (a) surface air temperature (1000 hPa), (b) specific humidity (1000 hPa) and (c) vertical velocity (1000 hPa) in the period 1950–2019 over Central China. The fitted average is marked by the red curve, depicting the interdecadal trend. (For interpretation of the references to colour in this figure legend, the reader is referred to the web version of this article.)

Tibetan Plateau. Although the meteorology-contributed ozone concentrations over Central China have been declined these years, our modeled summertime surface ozone data from CIMP6 are consistent with previous studies by observations and simulations, of a significant increasing

trend (Dentener et al., 2006; Avnery et al., 2011; Wang et al., 2017). These results indicate that the ozone increasing trend dependent on the changes of precursor emissions has intensified in these years over Central China, offsetting the ozone mitigation attributed to the climate change.

Data availability

NCEP/NCAR reanalysis data is downloaded from https://psl.noaa.gov/data/gridded/data.ncep.reanalysis.pressure.html/. ERA5 data is generated by European Centre for Medium-Range Weather Forecasts (https://www.ecmwf.int/en/forecasts/datasets/reanalysis-datasets/era5/). The modeled hourly surface ozone is from CMIP6 (https://cera-www.dkrz.de/WDCC/ui/cerasearch/cmip6?input=CMIP6.CMIP.MOHC.UKESM1-0-LL.historical/). Ozone satellite retrieval data of OMI is from https://www.cfa.harvard.edu/atmosphere/. The in-situ observation data is from the China's Ministry of Ecology and Environment (https://data.cma.cn/).

Declaration of Competing Interest

None.

Appendix A. Supplementary data

Supplementary data to this article can be found online at https://doi.org/10.1016/j.atmosres.2021.105735.

References

An, Z.S., Wu, G.X., Li, J.P., Sun, Y.B., Liu, Y.M., Zhou, W.J., Cai, Y.J., Duan, A.M., Li, L., Mao, J.Y., Cheng, H., Shi, Z.G., Tan, L.C., Yan, H., Ao, H., Chang, H., Feng, J., 2015. Global monsoon dynamics and climate change. In: Jeanloz, R., Freeman, K.H. (Eds.), Annual Review of Earth and Planetary Sciences, Vol 43, pp. 29–77. Annual Review of Earth and Planetary Sciences, Annual Reviews, Palo Alto.

Avnery, S., Mauzerall, D.L., Liu, J.F., Horowitz, L.W., 2011. Global crop yield reductions due to surface ozone exposure: 1. Year 2000 crop production losses and economic damage. Atmos. Environ. 45, 2284–2296. https://doi.org/10.1016/j.atmosenv.2010.11.045.

Bracegirdle, T.J., Marshall, G.J., 2012. The reliability of antarctic tropospheric pressure and temperature in the latest global reanalyses. J. Clim. 25, 7138–7146. https://doi.org/10.1175/jcli-d-11-00685.1.

Bromwich, D.H., Nicolas, J.P., Monaghan, A.J., 2011. An assessment of precipitation changes over Antarctica and the Southern Ocean since 1989 in contemporary global reanalyses. J. Clim. 24, 4189–4209. https://doi.org/10.1175/2011jcli4074.1.

Butler, A.H., Sjoberg, J.P., Seidel, D.J., Rosenlof, K.H., 2017. A sudden stratospheric warming compendium. Earth Syst. Sci. Data 9, 63–76. https://doi.org/10.5194/essd-9-63-2017.

Chen, X., Zhong, B.Q., Huang, F.X., Wang, X.M., Sarkar, S., Jia, S.G., Deng, X.J., Chen, D.H., Shao, M., 2020. The role of natural factors in constraining long-term tropospheric ozone trends over Southern China. Atmos. Environ. 220, 11. https://doi.org/10.1016/j.atmosenv.2019.117060.

Cheng, N.L., Li, R.Y., Xu, C.X., Chen, Z.Y., Chen, D.L., Meng, F., Cheng, B.F., Ma, Z.C.A., Zhuang, Y., He, B., Gao, B.B., 2019. Ground ozone variations at an urban and a rural station in Beijing from 2006 to 2017: trend, meteorological influences and formation regimes. J. Clean. Prod. 235, 11–20. https://doi.org/10.1016/j.jclepro.2019.06.204.

Cui, Y.F., Duan, A.M., Liu, Y.M., Wu, G.X., 2015. Interannual variability of the spring atmospheric heat source over the Tibetan Plateau forced by the North Atlantic SSTA. Clim. Dyn. 45, 1617–1634. https://doi.org/10.1007/s00382-014-2417-9.

Davies, T.D., Kelly, P.M., Low, P.S., Pierce, C.E., 1992. Surface ozone concentrations in Europe - links with the regional-scale atmospheric circulation. J. Geophys. Res.-Atmos. 97, 9819–9832. https://doi.org/10.1029/92jd00419.

Decker, M., Brunke, M.A., Wang, Z., Sakaguchi, K., Zeng, X.B., Bosilovich, M.G., 2012. Evaluation of the reanalysis products from GSFC, NCEP, and ECMWF using flux tower observations. J. Clim. 25, 1916–1944. https://doi.org/10.1175/jcli-d-11-00004.1.

Dentener, F., Stevenson, D., Ellingsen, K., Van Noije, T., Schultz, M., Amann, M., Atherton, C., Bell, N., Bergmann, D., Bey, I., Bouwman, L., Butler, T., Cofala, J., Collins, B., Drevet, J., Doherty, R., Eickhout, B., Eskes, H., Fiore, A., Gauss, M., Hauglustaine, D., Horowitz, L., Isaksen, I.S.A., Josse, B., Lawrence, M., Krol, M., Lamarque, J.F., Montanaro, V., Muller, J.F., Peuch, V.H., Pitari, G., Pyle, J., Rast, S., Rodriguez, I., Sanderson, M., Savage, N.H., Shindell, D., Strahan, S., Szopa, S., Sudo, K., Van Dingenen, R., Wild, O., Zeng, G., 2006. The global atmospheric environment for the next generation. Environ. Sci. Technol. 40, 3586–3594. https://doi.org/10.1021/es0523845.

Ding, Y.H., Chan, J.C.L., 2005. The East Asian summer monsoon: an overview. Meteorog. Atmos. Phys. 89, 117–142. https://doi.org/10.1007/s00703-005-0125-z.

Ding, Y.H., Wang, Z.Y., Sun, Y., 2008. Inter-decadal variation of the summer precipitation in East China and its association with decreasing Asian summer monsoon. Part I: Observed evidences. Int. J. Climatol. 28, 1139–1161. https://doi.org/10.1002/joc.1615.

Duan, A.M., Wu, G.X., 2005. Role of the Tibetan Plateau thermal forcing in the summer climate patterns over subtropical Asia. Clim. Dyn. 24, 793–807. https://doi.org/10.1007/s00382-004-0488-8.

Duan, J.C., Tan, J.H., Yang, L., 2008. Concentration, sources and ozone formation potential of volatile organic compounds (VOCs) during ozone episode in Beijing. Atmos. Res. 88, 25–35. https://doi.org/10.1016/j.atmosres.2007.09.004.

Duan, A.M., Li, F., Wang, M.R., Wu, G.X., 2011. Persistent weakening trend in the spring sensible heat source over the Tibetan Plateau and its impact on the Asian summer monsoon. J. Clim. 24, 5671–5682. https://doi.org/10.1175/jcli-d-11-00052.1.

Emberson, L., 2020. Effects of ozone on agriculture, forests and grasslands. Philos. Trans. R. Soc. A-Math. Phys. Eng. Sci. 378, 27. https://doi.org/10.1098/rsta.2019.0327.

Fu, Y., Tai, A.P.K., 2015. Impact of climate and land cover changes on tropospheric ozone air quality and public health in East Asia between 1980 and 2010. Atmos. Chem. Phys. 15, 10093–10106. https://doi.org/10.5194/acp-15-10093-2015.

Garreaud, R., Lopez, P., Minvielle, M., Rojas, M., 2013. Large-scale control on the Patagonian climate. J. Clim. 26, 215–230. https://doi.org/10.1175/jcli-d-12-00001.1.

Ge, J., You, Q.L., Zhang, Y.Q., 2019. Effect of Tibetan Plateau heating on summer extreme precipitation in eastern China. Atmos. Res. 218, 364–371. https://doi.org/10.1016/j.atmosres.2018.12.018.

Gong, C., Liao, H., 2019. A typical weather pattern for ozone pollution events in North China. Atmos. Chem. Phys. 19, 13725–13740. https://doi.org/10.5194/acp-19-13725-2019.

Griffiths, P.T., Murray, L.T., Zeng, G., Archibald, A.T., Emmons, L.K., Galbally, I., Hassler, B., Horowitz, L.W., Keeble, J., Liu, J., Moeini, O., Naik, V., O'Connor, F.M., Shin, Y.M., Tarasick, D., Tilmes, S., Turnock, S.T., Wild, O., Young, P.J., Zanis, P., 2021. Tropospheric ozone in CMIP6 Simulations. Atmos. Chem. Phys. Discuss. https://doi.org/10.5194/acp-2019-1216.

Han, H., Liu, J.E., Shu, L., Wang, T.J., Yuan, H.L., 2020. Local and synoptic meteorological influences on daily variability in summertime surface ozone in eastern China. Atmos. Chem. Phys. 20, 203–222. https://doi.org/10.5194/acp-20-203-2020.

Harris, N., 2006. The elevation history of the Tibetan Plateau and its implications for the Asian monsoon. Palaeogeogr. Palaeoclimatol. Palaeoecol. 241, 4–15. https://doi.org/10.1016/j.palaeo.2006.07.009.

He, J.J., Gong, S.L., Yu, Y., Yu, L.J., Wu, L., Mao, H.J., Song, C.B., Zhao, S.P., Liu, H.L., Li, X.Y., Li, R.P., 2017. Air pollution characteristics and their relation to meteorological conditions during 2014-2015 in major Chinese cities. Environ. Pollut. 223, 484–496. https://doi.org/10.1016/j.envpol.2017.01.050.

Jacob, D.J., Winner, D.A., 2009. Effect of climate change on air quality. Atmos. Environ. 43, 51–63. https://doi.org/10.1016/j.atmosenv.2008.09.051.

Jiang, F., Zhou, P., Liu, Q., Wang, T.J., Zhuang, B.L., Wang, X.Y., 2012. Modeling tropospheric ozone formation over East China in springtime. J. Atmos. Chem. 69, 303–319. https://doi.org/10.1007/s10874-012-9244-3.

Kavassalis, S.C., Murphy, J.G., 2017. Understanding ozone-meteorology correlations: a role for dry deposition. Geophys. Res. Lett. 44, 2922–2931. https://doi.org/10.1002/2016gl071791.

Krupa, S.V., Manning, W.J., 1988. Atmospheric ozone: formation and effects on vegetation. Environ. Pollut. (Barking, Essex : 1987) 50, 101–137. https://doi.org/10.1016/0269-7491(88)90187-x.

Lau, W.K.M., Kim, M.K., Kim, K.M., Lee, W.S., 2010. Enhanced surface warming and accelerated snow melt in the Himalayas and Tibetan Plateau induced by absorbing aerosols. Environ. Res. Lett. 5, 10. https://doi.org/10.1088/1748-9326/5/2/025204.

Lelieveld, J., Evans, J.S., Fnais, M., Giannadaki, D., Pozzer, A., 2015. The contribution of outdoor air pollution sources to premature mortality on a global scale. Nature 525, 367. https://doi.org/10.1038/nature15371.

Li, Q., Zhang, R.H., Wang, Y., 2016. Interannual variation of the wintertime fog-haze days across central and eastern China and its relation with East Asian winter monsoon. Int. J. Climatol. 36, 346–354. https://doi.org/10.1002/joc.4350.

Li, K., Jacob, D.J., Shen, L., Lu, X., De Smedt, I., Liao, H., 2020. Increases in surface ozone pollution in China from 2013 to 2019: anthropogenic and meteorological influences. Atmos. Chem. Phys. 20, 11423–11433. https://doi.org/10.5194/acp-20-11423-2020.

Liao, Z.H., Gao, M., Sun, J.R., Fan, S.J., 2017. The impact of synoptic circulation on air quality and pollution-related human health in the Yangtze River Delta region. Sci. Total Environ. 607, 838–846. https://doi.org/10.1016/j.scitotenv.2017.07.031.

Liu, Y.M., Bao, Q., Duan, A.M., Qian, Z.A., Wu, G.X., 2007. Recent progress in the impact of the Tibetan Plateau on climate in China. Adv. Atmos. Sci. 24, 1060–1076. https://doi.org/10.1007/s00376-007-1060-3.

Liu, X.D., Cheng, Z.G., Yan, L.B., 2009. Elevation dependency of recent and future minimum surface air temperature trends in the Tibetan Plateau and its surroundings. Glob. Planet. Chang. 68, 164–174. https://doi.org/10.1016/j.gloplacha.2009.03.017.

Ma, J.Z., Xu, X.B., Zhao, C.S., Yan, P., 2012. A review of atmospheric chemistry research in China: photochemical smog, haze pollution, and gas-aerosol interactions. Adv. Atmos. Sci. 29, 1006–1026. https://doi.org/10.1007/s00376-012-1188-7.

Ma, Z.Q., Xu, J., Quan, W.J., Zhang, Z.Y., Lin, W.L., Xu, X.B., 2016. Significant increase of surface ozone at a rural site, north of eastern China. Atmos. Chem. Phys. 16, 3969–3977. https://doi.org/10.5194/acp-16-3969-2016.

Parker, D.E., 2011. Recent L and surface air temperature trends assessed using the 20th century reanalysis. J. Geophys. Res.-Atmos. 116 https://doi.org/10.1029/2011jd016438.

Pepin, N., Bradley, R.S., Diaz, H.F., Baraer, M., Caceres, E.B., Forsythe, N., Fowler, H., Greenwood, G., Hashmi, M.Z., Liu, X.D., Miller, J.R., Ning, L., Ohmura, A., Palazzi, E., Rangwala, I., Schoner, W., Severskiy, I., Shahgedanova, M., Wang, M.B., Williamson, S.N., Yang, D.Q., Mt Res Initiative, E. D. W. W. G., 2015. Elevation-dependent warming in mountain regions of the world. Nat. Clim. Chang. 5, 424–430. https://doi.org/10.1038/nclimate2563.

Pu, X., Wang, T.J., Huang, X., Melas, D., Zanis, P., Papanastasiou, D.K., Poupkou, A., 2017. Enhanced surface ozone during the heat wave of 2013 in Yangtze River Delta region, China. Sci. Total Environ. 603, 807–816. https://doi.org/10.1016/j.scitotenv.2017.03.056.

Rodwell, M.J., Hoskins, B.J., 2010. Monsoons and the dynamics of deserts. Q. J. R. Meteorol. Soc. 122, 1385–1404. https://doi.org/10.1002/qj.49712253408.

Seo, J., Park, D.-SR., Kim, J.Y., Youn, D., Lim, Y.B., Kim, Y., 2018. Effects of meteorology and emissions on urban air quality: a quantitative statistical approach to long-term records (1999–2016) in Seoul, South Korea. Atmos. Chem. Phys. 18 (21), 16121–16137. https://doi.org/10.5194/acp-18-16121-2018.

Shen, L., Jacob, D.J., Liu, X., Huang, G.Y., Li, K., Liao, H., Wang, T., 2019. An evaluation of the ability of the Ozone Monitoring Instrument (OMI) to observe boundary layer ozone pollution across China: application to 2005-2017 ozone trends. Atmos. Chem. Phys. 19, 6551–6560. https://doi.org/10.5194/acp-19-6551-2019.

Shen, L.J., Zhao, T.L., Wang, H.L., Liu, J., Bai, Y.Q., Kong, S.F., Zheng, H., Zhu, Y., Shu, Z.Z., 2021. Importance of meteorology in air pollution events during the city lockdown for COVID-19 in Hubei Province. Central China, Sci. Total Environ. 754 https://doi.org/10.1016/j.scitotenv.2020.142227.

Shi, X.Y., Wang, Y.Q., Xu, X.D., 2008. Effect of mesoscale topography over the Tibetan Plateau on summer precipitation in China: a regional model study. Geophys. Res. Lett. 35, 19707–19711. https://doi.org/10.1029/2008GL034740.

Shu, L., Xie, M., Wang, T.J., Gao, D., Chen, P.L., Han, Y., Li, S., Zhuang, B.L., Li, M.M., 2016. Integrated studies of a regional ozone pollution synthetically affected by subtropical high and typhoon system in the Yangtze River Delta region, China. Atmos. Chem. Phys. 16, 15801–15819. https://doi.org/10.5194/acp-16-15801-2016.

Sillman, S., Logan, J.A., Wofsy, S.C., 1990. The sensitivity of ozone to nitrogen-oxides and hydrocarbons in regional ozone episodes. J. Geophys. Res.-Atmos. 95, 1837–1851. https://doi.org/10.1029/JD095iD02p01837.

Sun, L., Xue, L.K., Wang, Y.H., Li, L.L., Lin, J.T., Ni, R.J., Yan, Y.Y., Chen, L.L., Li, J., Zhang, Q.Z., Wang, W.X., 2019. Impacts of meteorology and emissions on summertime surface ozone increases over central eastern China between 2003 and 2015. Atmos. Chem. Phys. 19, 1455–1469. https://doi.org/10.5194/acp-19-1455-2019.

Tai, A.P.K., Martin, M.V., Heald, C.L., 2014. Threat to future global food security from climate change and ozone air pollution. Nat. Clim. Chang. 4, 817–821. https://doi.org/10.1038/nclimate2317.

Wang, B., Bao, Q., Hoskins, B.J., Wu, G.X., Liu, Y.M., 2008a. Tibetan Plateau warming and precipitation changes in East Asia. Geophys. Res. Lett. 35, 14702–14706. https://doi.org/10.1029/2008GL034330.

Wang, B., Wu, Z.W., Li, J.P., Liu, J., Chang, C.P., Ding, Y.H., Wu, G.X., 2008b. How to measure the strength of the East Asian summer monsoon. J. Clim. 21, 4449–4463. https://doi.org/10.1175/2008JCLI2183.1.

Wang, Y.B., Liu, X.Q., Herzschuh, U., 2010. Asynchronous evolution of the Indian and East Asian summer monsoon indicated by Holocene moisture patterns in monsoonal Central Asia. Earth-Sci. Rev. 103, 135–153. https://doi.org/10.1016/j.earscirev.2010.09.004.

Wang, Z.Q., Duan, A.M., Wu, G.X., 2014. Time-lagged impact of spring sensible heat over the Tibetan Plateau on the summer rainfall anomaly in East China: case studies using the WRF model. Clim. Dyn. 42, 2885–2898. https://doi.org/10.1007/s00382-013-1800-2.

Wang, T., Xue, L.K., Brimblecombe, P., Lam, Y.F., Li, L., Zhang, L., 2017. Ozone pollution in China: a review of concentrations, meteorological influences, chemical precursors, and effects. Sci. Total Environ. 575, 1582–1596. https://doi.org/10.1016/j.scitotenv.2016.10.081.

Wie, J., Moon, B.K., 2016. Seasonal relationship between meteorological conditions and surface ozone in Korea based on an offline chemistry-climate model. Atmos. Pollut. Res. 7, 385–392. https://doi.org/10.1016/j.apr.2015.10.020.

Woollings, T., Franzke, C., Hodson, D.L.R., Dong, B., Barnes, E.A., Raible, C.C., Pinto, J. G., 2015. Contrasting interannual and multidecadal NAO variability. Clim. Dyn. 45, 539–556. https://doi.org/10.1007/s00382-014-2237-y.

Wu, G.X., Liu, Y., Wang, T.M., Wan, R.J., Liu, X., Li, W.P., Wang, Z.Z., Zhang, Q., Duan, A.M., Liang, X.Y., 2007. The influence of mechanical and thermal forcing by the Tibetan Plateau on Asian climate. J. Hydrometeorol. 8, 770–789. https://doi.org/10.1175/JHM609.1.

Wu, G.X., Zhuo, H.I., Wang, Z.Q., Liu, Y.M., 2016. Two types of summertime heating over the Asian large-scale orography and excitation of potential-vorticity forcing I. Over Tibetan Plateau. Sci. China-Earth Sci. 59, 1996–2008. https://doi.org/10.1007/s11430-016-5328-2.

Wu, G.X., He, B., Duan, A.M., Liu, Y.M., Yu, W., 2017. Formation and variation of the atmospheric heat source over the Tibetan Plateau and its climate effects. Adv. Atmos. Sci. 34, 1169–1184. https://doi.org/10.1007/s00376-017-7014-5.

Xu, X., Lin, W., 2011. Trends of tropospheric ozone over China based on satellite data (1979e2005). Adv. Clim. Chang. Res. 2, 43–48.

Xu, X.D., Lu, C.G., Ding, Y.H., Shi, X.H., Guo, Y.D., Zhu, W.H., 2013. What is the relationship between China summer precipitation and the change of apparent heat source over the Tibetan Plateau? Atmos. Sci. Lett. 14, 227–234. https://doi.org/10.1002/asl2.444.

Xu, X., Zhao, T., Liu, F., Gong, S.L., Kristovich, D., Lu, C., Guo, Y., Cheng, X., Wang, Y., Ding, G., 2016. Climate modulation of the Tibetan Plateau on haze in China. Atmos. Chem. Phys. 16, 1365–1375. https://doi.org/10.5194/acp-16-1365-2016.

Xu, W.Y., Xu, X.B., Lin, M.Y., Lin, W.L., Tarasick, D., Tang, J., Ma, J.Z., Zheng, X.D., 2018. Long-term trends of surface ozone and its influencing factors at the Mt Waliguan GAW station, China - part 2: the roles of anthropogenic emissions and climate variability. Atmos. Chem. Phys. 18, 773–798. https://doi.org/10.5194/acp-18-773-2018.

Yan, Y.Y., Lin, J.T., He, C.L., 2018a. Ozone trends over the United States at different times of day. Atmos. Chem. Phys. 18, 1185–1202. https://doi.org/10.5194/acp-18-1185-2018.

Yan, Y.Y., Pozzer, A., Ojha, N., Lin, J.T., Lelieveld, J., 2018b. Analysis of European ozone trends in the period 1995-2014. Atmos. Chem. Phys. 18, 5589–5605. https://doi.org/10.5194/acp-18-5589-2018.

Yan, Y.Y., Lin, J.T., Pozzer, A., Kong, S.F., Lelieveld, J., 2019. Trend reversal from high-to-low and from rural-to-urban ozone concentrations over Europe. Atmos. Environ. 213, 25–36. https://doi.org/10.1016/j.atmosenv.2019.05.067.

Yan, Y.Y., Zheng, H., Kong, S.F., Lin, J.T., Yao, L.Q., Wu, F.Q., Cheng, Y., Niu, Z.Z., Zheng, S.R., Zeng, X., Yan, Q., Wu, J., Zheng, M.M., Liu, M.Y., Ni, R.J., Chen, L.L., Chen, N., Xu, K., Liu, D.T., Zhao, D.L., Zhao, T.L., Qi, S.H., 2021. On the local anthropogenic source diversities and transboundary transport for urban agglomeration ozone mitigation. Atmos. Environ. 245, 11. https://doi.org/10.1016/j.atmosenv.2020.118005.

Yang, Y., Liao, H., Li, J., 2014a. Impacts of the East Asian summer monsoon on interannual variations of summertime surface-layer ozone concentrations over China. Atmos. Chem. Phys. 14, 6867–6879. https://doi.org/10.5194/acp-14-6867-2014.

Yang, K., Wu, H., Qin, J., Lin, C.G., Tang, W.J., Chen, Y.Y., 2014b. Recent climate changes over the Tibetan Plateau and their impacts on energy and water cycle: a review. Glob. Planet. Chang. 112, 79–91. https://doi.org/10.1016/j.gloplacha.2013.12.001.

Yu, C., Zhao, T.L., Bai, Y.Q., Zhang, L., Kong, S.F., Yu, X.N., He, J.H., Cui, C.G., Yang, J., You, Y.C., Ma, G.X., Wu, M., Chang, J.C., 2020. Heavy air pollution with a unique "non-stagnant" atmospheric boundary layer in the Yangtze River middle basin aggravated by regional transport of PM2.5 over China. Atmos. Chem. Phys. 20, 7217–7230. https://doi.org/10.5194/acp-20-7217-2020.

Zeng, P., Lyu, X.P., Guo, H., Cheng, H.R., Jiang, F., Pan, W.Z., Wang, Z.W., Liang, S.W., Hu, Y.Q., 2018. Causes of ozone pollution in summer in Wuhan, Central China. Environ. Pollut. 241, 852–861. https://doi.org/10.1016/j.envpol.2018.05.042.

Zhang, J.P., Zhu, T., Zhang, Q.H., Li, C.C., Shu, H.L., Ying, Y., Dai, Z.P., Wang, X., Liu, X.Y., Liang, A.M., Shen, H.X., Yi, B.Q., 2012. The impact of circulation patterns on regional transport pathways and air quality over Beijing and its surroundings. Atmos. Chem. Phys. 12, 5031–5053. https://doi.org/10.5194/acp-12-5031-2012.

Zhang, J.K., Tian, W.S., Wang, Z.W., Xie, F., Wang, F.Y., 2015. The influence of ENSO on Northern Midlatitude ozone during the winter to spring transition. J. Clim. 28, 4774–4793. https://doi.org/10.1175/jcli-d-14-00615.1.

Zhang, Y., Yin, Z., Wang, H., 2020. Roles of climate variability on the rapid increases of early winter haze pollution in North China after 2010. Atmos. Chem. Phys. 20, 12211–12221. https://doi.org/10.5194/acp-20-12211-2020.

Zhao, P., Chen, L.X., 2001. Climatic features of atmospheric heat source/sink over the Qinghai-Xizang Plateau in 35 years and its relation to rainfall in China. Sci. in China (Series D) 44, 92–98. CNKI:SUN:JDXG.0.2001–09-009.

Zhao, P., Zhou, Z.J., Liu, J.P., 2007. Variability of Tibetan spring snow and its associations with the hemispheric extratropical circulation and East Asian summer monsoon rainfall: an observational investigation. J. Clim. 20, 3942–3955. https://doi.org/10.1175/JCLI4205.1.

Zhao, S.Y., Feng, T., Tie, X.X., Wang, Z.B., 2020. The warming Tibetan Plateau improves winter air quality in the Sichuan Basin, China. Atmos. Chem. Phys. 20, 14873–14887. https://doi.org/10.5194/acp-20-14873-2020.

Zheng, H., Kong, S.F., Wu, F.Q., Cheng, Y., Niu, Z.Z., Zheng, S.R., Yang, G.W., Yao, L.Q., Yan, Q., Wu, J., Zheng, M.M., Chen, N., Xu, K., Yan, Y.Y., Liu, D.T., Zhao, D.L., Zhao, T.L., Bai, Y.Q., Li, S.L., Qi, S.H., 2019. Intra-regional transport of black carbon between the south edge of the North China Plain and Central China during winter haze episodes. Atmos. Chem. Phys. 19, 4499–4516. https://doi.org/10.5194/acp-19-4499-2019.

Zhou, X.J., Zhao, P., Chen, J.M., Chen, L.X., Li, W.L., 2009. Impacts of thermodynamic processes over the Tibetan Plateau on the Northern Hemispheric climate. Sci. China Ser. D Earth Sci. 52, 1679–1693. https://doi.org/10.1007/s11430-009-0194-9.

Zhou, D.R., Ding, A.J., Mao, H.T., Fu, C.B., Wang, T., Chan, L.Y., Ding, K., Zhang, Y., Liu, J., Lu, A., Hao, N., 2013. Impacts of the East Asian monsoon on lower tropospheric ozone over coastal South China. Environ. Res. Lett. 8, 7. https://doi.org/10.1088/1748-9326/8/4/044011.